

Synthesis and Characterization of Magnesium-Aluminum Layered Double Hydroxides Containing (Tetrasulfonated porphyrin)cobalt

César A. S. Barbosa,^[a] Ana Maria D. C. Ferreira,^[a] and Vera R. L. Constantino*^[a]

Keywords: Composites / Intercalations / Layered compounds / Organic–inorganic hybrid composites / Porphyrins

We report the synthesis and characterization of a magnesium-aluminum layered double hydroxide (LDH) containing [5,10,15,20-tetrakis(4-sulfonatophenyl)porphyrinato]cobalt(II) (CoTPhsP) by two routes: (i) CoTPhsP intercalation by structure reconstruction of the calcined pristine LDH [Mg_{2.8}Al-(CoTPhsP)_{int}] and (ii) adsorption of the CoTPhsP on the external surfaces of the noncalcined pristine LDH [Mg_{3.0}Al-(CoTPhsP)_{ads}]. The intercalation and adsorption of CoTPhsP in the LDHs were evaluated using different techniques, such as X-ray diffraction, thermogravimetry, scanning electronic microscopy, and surface area and porosity analysis. Further characterization by electron spin resonance and UV/Vis spectroscopy showed that the CoTPhsP molecules adsorbed and intercalated in the LDHs are present as two predominant species: the complex formed with molecular oxygen (CoTPhsP–O₂) and the corresponding deoxy monomeric species (CoTPhsP). The stability and reactivity of the CoTPhsP

immobilized in the LDHs were evaluated in the presence of hydrogen peroxide solution. CoTPhsP in homogeneous conditions is deactivated by molecular aggregation and/or oxidative self-destruction in the presence of H₂O₂. On the other hand, CoTPhsP stability and reactivity were improved when adsorbed and intercalated in the LDHs. Mg_{3.0}Al(CoTPhsP)_{ads} is more active than Mg_{2.8}Al(CoTPhsP)_{int} in the decomposition of hydrogen peroxide to H₂O and O₂. A porosity analysis carried out by N₂ adsorption-desorption experiments for the intercalated material exhibited a type-IV isotherm characteristic of nonmicroporous materials. Hence, the CoTPhsP molecules located in the LDH galleries are not accessible to the H₂O₂, while the metal centers in the Mg_{3.0}Al(CoTPhsP)_{ads} sample are more available, which may explain the enhanced reactivity.

(© Wiley-VCH Verlag GmbH & Co. KGaA, 69451 Weinheim, Germany, 2005)

Introduction

The intercalation of guest species in crystalline layered host matrices is considered to be a versatile synthetic method for the synthesis of nanostructured hybrid materials. The intercalated materials are particularly attractive because different synthetic approaches provide routes to tune the material properties by mediating the chemical composition of the host matrices and the intercalated species.^[1,2]

Among two-dimensional matrices, layered double hydroxides (LDHs) have been found to be an interesting system for intercalation of different species.^[3,4] The LDH composition is represented by the general formula [M^{II}_(1-x)M^{III}_x(OH)₂](Aⁿ⁻)_{x/n}·zH₂O, where Aⁿ⁻ is the interlayer anion and M^{II} and M^{III} are di- and trivalent metals, respectively, located in the positively charged brucite-like layers.^[5] LDHs with different compositions can be synthesized by varying the nature of M^{II}, M^{III}, and Aⁿ⁻. This versatility has allowed the isolation of LDH materials with varied functionalities, including their use as catalysts,^[6] reinforced fillers in organic polymers,^[7] ion-exchangers for environmental remediation,^[8] and, more recently, as drug^[9] and gene carriers.^[10]

Synthetic metalloporphyrins are a well-known class of macrocyclic complexes that have been widely studied as catalysts for organic reactions based on their selective activity in catalyzed oxidations by heme enzymes such as, for example, cytochrome P-450 and peroxidases.^[11] However, the reactivity of many synthetic metalloporphyrins is greatly reduced due to their molecular aggregation or oxidative self-destruction in the reaction media. In the presence of hydrogen peroxide these porphyrins are used for catalytic oxidation during important organic conversions due to the formation of a high-valent oxometal–porphyrin active complex.^[11] Nevertheless, synthetic metalloporphyrins can lead to the undesired homolytic cleavage of H₂O₂ with generation of hydroxyl radical (Fenton-type reaction), which is a strong, nonselective oxidant of organic substrates and can decompose the metalloporphyrin.^[12]

In order to overcome these disadvantages, synthetic metalloporphyrins have been immobilized in different inorganic and organic host networks.^[13] In addition to the improved stability and reactivity of the metalloporphyrin catalyst, the immobilization in host matrices has been pointed out as an interesting route for their “heterogenization”, facilitating the catalyst separation and recovery from the final reaction mixture.^[14]

Sulfonated and carboxylated metalloporphyrins intercalated into LDHs have been prepared by several synthetic

[a] Instituto de Química, Universidade de São Paulo, Caixa Postal 26077, CEP 05513-970 São Paulo, SP, Brazil
Fax: +55-11-3815-5579
E-mail: vrlconst@iq.usp.br

routes, with various M^{2+} and M^{3+} ions and molar ratios in the LDH composition, and also with different transition metals in the porphyrin core.^[15–22] Furthermore, nonmetallated anionic porphyrins have also been used to prepare intercalated LDHs.^[23–25] These nanostructured hybrid materials have shown interesting properties as catalysts in organic conversions,^[15,18,19] sensitizers in photochemical assemblies,^[16] and asymmetric charge-carriers for the development of solar-energy conversion devices.^[20]

We report in this work the synthesis of magnesium-aluminum LDHs containing [5,10,15,20-tetrakis(4-sulfonato-phenyl)porphyrinato]cobalt(II) (CoTPhsP) through two synthetic routes: (i) the structure reconstruction of the calcined $Mg_{3.0}Al(OH)_8.0(CO_3)_{0.5} \cdot xH_2O$ pristine LDH in the presence of the anionic porphyrin (reconstruction method); (ii) adsorption of the anionic metalloporphyrin onto the external surfaces of the pristine LDH (Figure 1). To the best of our knowledge this is the first report regarding the synthesis and characterization of CoTPhsP adsorbed in a magnesium-aluminum LDH and its successful intercalation into the inorganic matrix by the reconstruction method. The isolated materials were characterized by X-ray diffraction (XRD), surface area and porosity analysis, thermogravimetry (TGA), scanning electronic microscopy (SEM), electron spin resonance (ESR), and infrared (IR) and electronic (UV/Vis) spectroscopy. In addition, the stability and longevity of the immobilized porphyrins (adsorbed and intercalated in the LDHs) were evaluated in the presence of hydrogen peroxide.

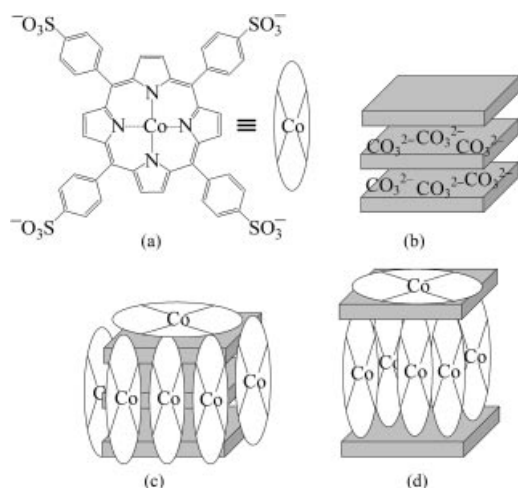


Figure 1. Schematic representation of CoTPhsP (a), $Mg_{3.0}Al-CO_3$ LDH (b) and idealized immobilization of CoTPhsP in the LDHs through adsorption (carbonate ions located between the layers are omitted for clarity) (c) or intercalation (d).

Results and Discussion

Materials Characterization

A typical XRD pattern was found for $Mg_{3.0}Al-CO_3$ prepared by coprecipitation (a profile similar to those presented by hydrotalcite-like compounds): sharp and symmet-

ric peaks related to 00 l reflections and broad and less symmetric peaks related to 0 kl reflections (Figure 2a). The peaks were indexed in a hexagonal cell with rhombohedral symmetry, where $c_0 = 23.4$ Å and $a_0 = 3.06$ Å. From the c_0 parameter, which corresponds to three times the distance between adjacent layers, an interlayer distance of 7.80 Å could be calculated, which is typical for hydrotalcite-like materials containing carbonate anions.^[26]

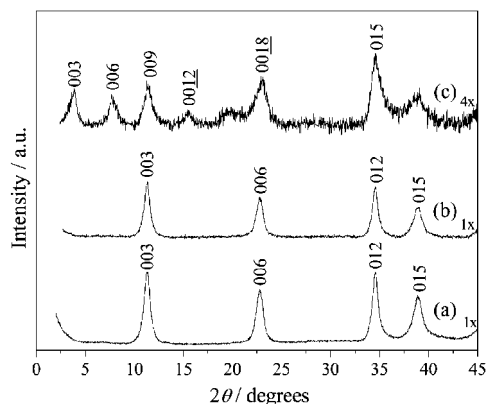


Figure 2. XRD patterns of $Mg_{3.0}Al-CO_3$ (a), $Mg_{3.0}Al(CoTPhsP)_{ads}$ (b), and $Mg_{2.8}Al(CoTPhsP)_{int}$ (c).

In relation to $Mg_{3.0}Al(CoTPhsP)_{ads}$ which contains the CoTPhsP adsorbed on the LDH external surfaces, the XRD pattern is identical to the $Mg_{3.0}Al-CO_3$ precursor (Figure 2b). This result shows, as expected, that the anionic porphyrin is not ion-exchanged with carbonate anions in the LDH.

The intercalated material isolated from the synthesis of $Mg_{2.8}Al(CoTPhsP)_{int}$ shows an XRD pattern different from the $Mg_{3.0}Al-CO_3$ precursor: a lower crystallinity and new peaks observed in the 2θ range 2.5–20° (Figure 2c).

Considering the same crystalline system used to assign the LDH precursor peaks, we find cell dimensions of $c_0 = 70.2$ Å and $a_0 = 3.06$ Å. The former corresponds to an interlayer distance of 23.4 Å. By comparing the interlayer distance between $Mg_{3.0}Al-CO_3$ and $Mg_{2.8}Al(CoTPhsP)_{int}$ one observes that the porphyrin incorporation expands the LDH layers by 15.6 Å. Moreover, by subtracting the LDH layer thickness (4.8 Å) from the interlayer distance, the gallery height of $Mg_{2.8}Al(CoTPhsP)_{int}$ is found to be equal to 18.6 Å, which is similar to the dimensions of the metalloporphyrin molecular plane (ca. 18×18 Å).^[23] These results indicate that CoTPhsP has been successfully intercalated in a perpendicular orientation to the LDH layers. Such a perpendicular arrangement has been observed for LDHs intercalated with anionic metalloporphyrins^[19,20] and non-metallated anionic porphyrins,^[23–25] using different synthetic methods.

Characterization by infrared spectroscopy indicates that CoTPhsP has been intercalated intact into the LDH. The IR spectra (not shown) of both neat and intercalated porphyrin exhibit similar characteristic absorption bands: 854, 885, and 1003 cm^{-1} (C–H pyrrole bending); 1290, 1348, and 1392 cm^{-1} (C–N stretching); 1495 and 1563 cm^{-1} (C–C

phenyl and pyrrole stretching, respectively); 1038, 1126, and 1186 cm^{-1} (sulfonic groups).^[27] In the IR spectra of $\text{Mg}_{2.8}\text{Al}(\text{CoTPhsP})_{\text{int}}$, we noticed some changes in the relative band intensities at 1330–1400 cm^{-1} . In this region, the minor changes are attributed to the carbonate ions present in the LDH interlayer (ν_3 vibrational mode of CO_3^{2-}).^[28] The hydroxide anion may also be present in the material, as it is formed in the LDH interlayer when using the reconstruction method^[29] during the CoTPhsP intercalation procedure. Hence, it is possible that $\text{Mg}_{2.8}\text{Al}(\text{CoTPhsP})_{\text{int}}$ contains, in addition to the porphyrin, hydroxide anions co-intercalated.

We have reported in a previous work that the intercalation of macrocyclic species in LDHs can lead to composites with an appreciable thermal stability.^[30] Moreover, the guest localization in the LDH results in materials with distinct thermal behavior. Similar results were found with the LDH containing intercalated CoTPhsP, according to the thermogravimetric curves of the samples shown in Figure 3.

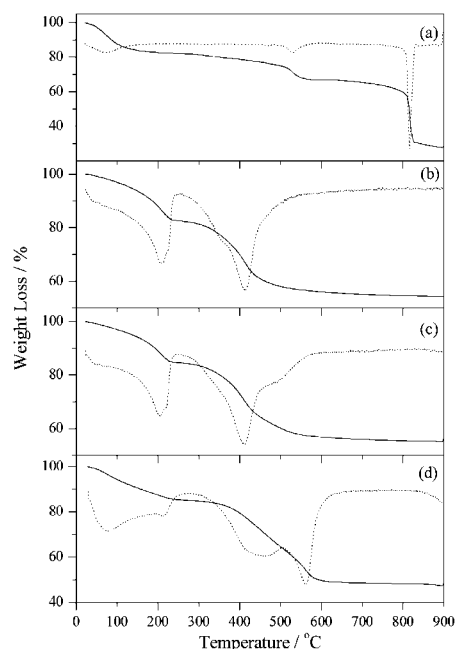


Figure 3. TGA (solid line) and DTG (dotted line) curves for CoTPhsP (sodium salt) (a), $\text{Mg}_{3.0}\text{Al-CO}_3$ (b), $\text{Mg}_{3.0}\text{Al}(\text{CoTPhsP})_{\text{ads}}$ (c), and $\text{Mg}_{2.8}\text{Al}(\text{CoTPhsP})_{\text{int}}$ (d).

The TG analysis of CoTPhsP shows a considerable thermal stability of the porphyrin (Figure 3a). A weight loss up to about 200 °C corresponds to the loss of hydration water.

The porphyrin decomposition seems to occur in two steps. The first step is observed at about 490 °C and the second one starts at about 625 °C, with the main weight loss occurring at 815 °C. Figure 3b shows the TG curve for the LDH carbonate. The first step of weight loss (up to 210 °C) is ascribed to the water release and the second one (above 300 °C) to the LDH dehydroxylation and decarbonation, as discussed previously.^[31]

The thermal behavior of $\text{Mg}_{3.0}\text{Al}(\text{CoTPhsP})_{\text{ads}}$ up to around 600 °C can be interpreted as an overlap of TG curves for neat CoTPhsP and $\text{Mg}_{3.0}\text{Al-CO}_3$ (Figure 3c). Nevertheless, the weight loss observed for CoTPhsP above 625 °C is not present in the TG curve of the adsorbed CoTPhsP. The thermal behavior of $\text{Mg}_{2.8}\text{Al}(\text{CoTPhsP})_{\text{int}}$ shows a higher stability towards decomposition of both the LDH matrix and CoTPhsP (Figure 3d). The dehydroxylation and decarbonation events seem to occur at about 330 °C, whereas the $\text{Mg}_{3.0}\text{Al-CO}_3$ LDH precursor decomposes at about 300 °C. The weight losses starting at 520 and 850 °C seem to be related to the decomposition of CoTPhsP, which suggests a higher stability than for neat CoTPhsP.

Textural characterization was performed by surface area and porosity measurements. $\text{Mg}_{3.0}\text{Al-CO}_3$ shows a surface area of 86 m^2g^{-1} . For $\text{Mg}_{2.8}\text{Al}(\text{CoTPhsP})_{\text{int}}$, the surface area of 34 m^2g^{-1} indicates that no micropores have been produced in the intercalation product as a substantial increase in the surface area compared to the LDH precursor would be expected if microporosity was present. This assumption was confirmed by N_2 adsorption-desorption isotherms of the sample. $\text{Mg}_{2.8}\text{Al}(\text{CoTPhsP})_{\text{int}}$ exhibits type-IV isotherms (not shown) characteristic of nonmicroporous materials with a hysteresis loop indicating interparticle mesoporosity, according to the IUPAC classification.^[32] We have previously observed similar results from the material isolated after intercalation of (phthalocyanine) Cu^{II} tetrasulfonate in the same LDH $\text{Mg}_{3.0}\text{Al}$ precursor.^[30] $\text{Mg}_{3.0}\text{Al}(\text{CoTPhsP})_{\text{ads}}$ shows a surface area of 106 m^2g^{-1} . This increase in the surface area related to the $\text{Mg}_{3.0}\text{Al-CO}_3$ does not, however, indicate microporosity in the material. As described before, the interlayer space is occupied by the carbonate ions whereas CoTPhsP molecules are adsorbed on the external surface of the LDH.

Scanning electron micrographs obtained from the samples revealed a different morphology in the LDH after CoTPhsP intercalation by the reconstruction method (Figure 4). The SEM image of $\text{Mg}_{3.0}\text{Al-CO}_3$ presents a typical

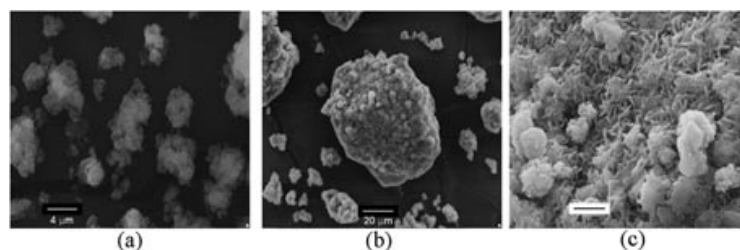


Figure 4. SEM images of $\text{Mg}_3\text{Al-CO}_3$ (10 000 \times) (a) and $\text{Mg}_{2.8}\text{Al}(\text{CoTPhsP})_{\text{int}}$ with different magnifications: 2000 \times (b) and 10 000 \times (c).

morphology expected for synthetic hydrotalcite-like compounds, with round particles of plate-like shapes (Figure 4a).

The adsorption of CoTPhsP on the external surface of the LDH layers results in a higher aggregation of the particles, which present the same morphology as observed for the LDH $\text{Mg}_{3.0}\text{Al}-\text{CO}_3$ (SEM image not shown). On the other hand, the intercalation of CoTPhsP into the LDH shows a distinct morphology (Figure 4b and Figure 4c). In the SEM images of $\text{Mg}_{2.8}\text{Al}(\text{CoTPhsP})_{\text{int}}$ we observed a new phase with stick-like particles, and also particles with a plate-like shape.

Information about the electronic properties of free and immobilized CoTPhsP in the LDHs was obtained by recording the ESR and UV/Vis spectra of the samples. Figure 5 shows the UV/Vis spectra for CoTPhsP in different solutions.

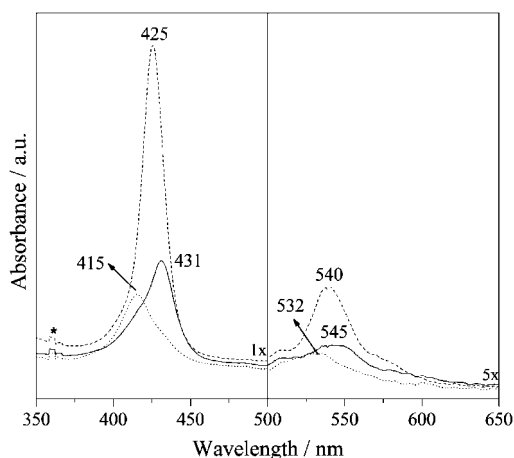


Figure 5. UV/Vis absorption spectra of 2 mmol L⁻¹ CoTPhsP in aqueous solution (dashed line), in 90% DMF/10% water solution (solid line), and the latter solution after the addition of sodium dithionite (dotted line). Further details are provided in the text. The feature indicated by an asterisk is an instrument artifact.

The UV/Vis spectrum of CoTPhsP in aqueous solution shows the characteristic bands for metalloporphyrins, dominated by $\pi-\pi^*$ transitions, located at 425 nm (Soret band) and 540 and 580 nm (Q bands).^[33] The presence of *N,N*-dimethylformamide (DMF), a coordinating solvent, results in a decrease in the intensity of both Soret and Q bands, accompanied by a small red shift (ca. 5 nm). The ESR spectra for 2 mmol L⁻¹ CoTPhsP solutions were recorded for the assignment of the porphyrin species. An aqueous solution of this metalloporphyrin is ESR-silent, as previously reported in the literature.^[34] The ESR spectrum of CoTPhsP in 90% DMF/10% water is shown in Figure 6a.

CoTPhsP is a low-spin Co^{II} complex with the single unpaired electron in the d_{z^2} orbital pointing out of the porphyrin plane.^[35] This configuration makes the unpaired electron very sensitive to changes in the axial coordination of the metal ion, which makes the ESR technique useful for studying Co^{II}-porphyrins.^[34–39] According to the literature,^[34,36,39] CoTPhsP in water does not give an ESR signal

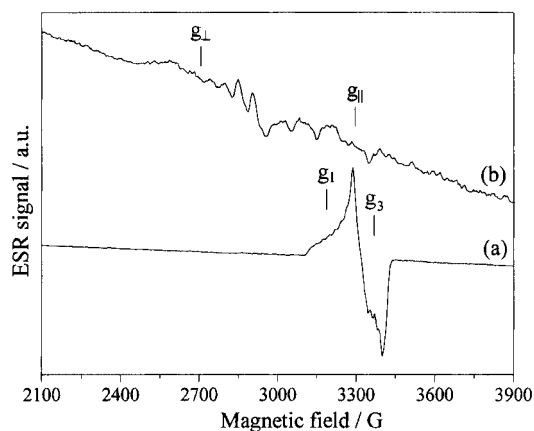


Figure 6. ESR spectra, recorded at 77 K, of 2 mmol L⁻¹ CoTPhsP in 90% DMF/10% water solution (a) and after addition of sodium dithionite (b). Further details are provided in the text.

due to aggregation of the metalloporphyrin molecules and/or formation of a diamagnetic μ -peroxo complex with molecular oxygen ($\text{CoTPhsP}-\text{O}_2-\text{CoTPhsP}$). The addition of DMF causes deaggregation, resulting in a solution containing the monomeric species of the CoTPhsP. The resulting ESR spectra, as reported by de Bolfo et al.,^[34] should present a characteristic signal with $g_{\parallel} = 2.040$ ($A_{\parallel} = 95 \times 10^{-4} \text{ cm}^{-1}$) and $g_{\perp} = 2.410$ ($A_{\perp} = 43 \times 10^{-4} \text{ cm}^{-1}$). In addition to the CoTPhsP monomeric species, a second ESR signal may be observed due to the complex formed by the metalloporphyrin with molecular oxygen ($\text{Co}^{\text{II}}\text{TPhsP}-\text{O}_2$) with $g_1 = 2.088$ ($A_1 = 22 \times 10^{-4} \text{ cm}^{-1}$), $g_2 = 1.998$ ($A_2 = 8 \times 10^{-4} \text{ cm}^{-1}$), and $g_3 = 1.997$ ($A_3 = 16 \times 10^{-4} \text{ cm}^{-1}$). The $\text{CoTPhsP}-\text{O}_2$ complex has also been detected for other cobalt-porphyrins.^[35,39] The structure of this complex is also represented by $\text{Co}^{\text{III}}\text{TPhsP}-\text{O}_2^-$ (superoxo complex) because the low values of hyperfine coupling in the ESR suggest that the unpaired electron resides primarily on the oxygen molecule.^[37]

As shown in Figure 6a, the ESR spectrum for CoTPhsP in 90% DMF/10% water solution shows a signal at around 3300 G with $g_1 = 2.090$ ($A_1 = 21.7 \times 10^{-4} \text{ cm}^{-1}$) and $g_3 = 1.997$ ($A_3 = 15.8 \times 10^{-4} \text{ cm}^{-1}$) (g_2 factor and A_2 unresolved in the spectrum). This signal is attributed to the $\text{CoTPhsP}-\text{O}_2$ complex as the g factor and hyperfine-coupling values are in agreement with those reported by de Bolfo et al.^[34] However, the monomeric ESR signal is not present in the spectrum of the CoTPhsP in solution. According to de Bolfo et al., a solid sample of CoTPhsP stored for a long time in air gives rise to an ESR spectrum showing only the $\text{CoTPhsP}-\text{O}_2$ signal, even when this stored sample was dissolved in aqueous solution containing different organic solvents.^[34] Indeed, the CoTPhsP sample used in the present study was stored for more than six months without protection from atmospheric air. In an attempt to record the ESR spectra of the monomeric species, oxygen was removed from the 2 mmol L⁻¹ CoTPhsP solution in 90% DMF/10% water solution by adding a small amount of sodium dithionite. Indeed, the ESR spectrum (Figure 6b) of this solution

did not show the CoTPhsP–O₂ signal and a new one appeared, which is related to the monomeric species, with $g_{\parallel} = 2.029$ ($A_{\parallel} = 91.2 \times 10^{-4} \text{ cm}^{-1}$) and $g_{\perp} = 2.455$ ($A_{\perp} = 52 \times 10^{-4} \text{ cm}^{-1}$). The UV/Vis spectrum of this deoxygenated CoTPhsP solution shows Soret and Q bands at 415 and 532 nm, respectively, with a blue shift in comparison to the spectrum for the solution containing the CoTPhsP–O₂ complex (Figure 5).

Based on the ESR spectra recorded for free CoTPhsP, we suggest that the UV/Vis absorption bands at 425 and 540 nm for the metalloporphyrin in aqueous solution can be assigned to the CoTPhsP–O₂–CoTPhsP complex, whereas in 90% DMF/10% water solution, the bands at 431 and 545 nm can be assigned to the CoTPhsP–O₂ complex. The bands observed at 415 and 532 nm, after addition of sodium dithionite to the latter solution, can be attributed to the CoTPhsP monomeric species. In light of these findings, $\text{Mg}_{3.0}\text{Al}(\text{CoTPhsP})_{\text{ads}}$ and $\text{Mg}_{2.8}\text{Al}(\text{CoTPhsP})_{\text{int}}$ were next examined by recording the UV/Vis (Figure 7) and ESR spectra (Figure 8) of these samples.

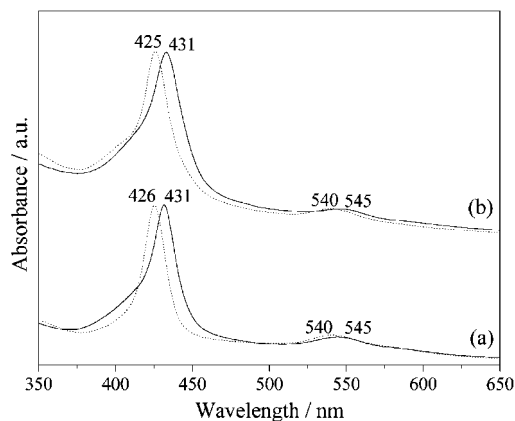


Figure 7. UV/Vis absorption spectra for $\text{Mg}_{2.8}\text{Al}(\text{CoTPhsP})_{\text{int}}$ (a) and $\text{Mg}_{3.0}\text{Al}(\text{CoTPhsP})_{\text{ads}}$ (b) solid samples dispersed in deionized water (dotted line) and 90% DMF/10% water solution (solid line).

The UV/Vis spectra for $\text{Mg}_{3.0}\text{Al}(\text{CoTPhsP})_{\text{ads}}$ and $\text{Mg}_{2.8}\text{Al}(\text{CoTPhsP})_{\text{int}}$ dispersed in deionized water and 90% DMF/10% water solution show a prominent broadening and a shoulder at around 410 nm in relation to neat CoTPhsP in the same solvents (Figure 5), although the Soret and Q band positions remain unchanged. Furthermore, the Soret band peak intensity decreases in relation to the Q band peak. Similar spectral profiles have also been observed in the electronic spectra of sulfonated metalloporphyrins^[17,19–21] and nonmetallated sulfonated porphyrins intercalated in different LDHs,^[23,24] which were ascribed to the aggregation of the porphyrin.^[40,41] However, considering the ESR and UV/Vis spectra recorded for CoTPhsP in deionized water and in DMF/water solutions, we suggest that this broadening and the shoulder around 410 nm for the Soret band in $\text{Mg}_{3.0}\text{Al}(\text{CoTPhsP})_{\text{ads}}$ and $\text{Mg}_{2.8}\text{Al}(\text{CoTPhsP})_{\text{int}}$ are related to the different CoTPhsP species present in the LDHs. The main absorption bands are related to the CoTPhsP–O₂ complex (for dispersion in DMF/water) or the CoTPhsP–O₂–CoTPhsP species (for disper-

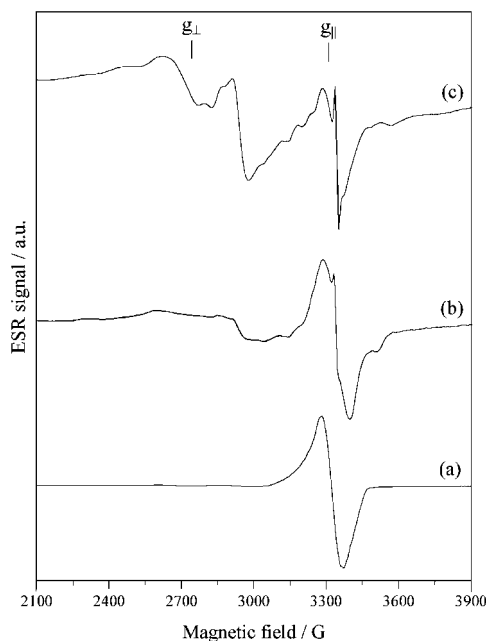


Figure 8. Powder ESR spectra, recorded at 77 K, of CoTPhsP (sodium salt) (a), $\text{Mg}_{3.0}\text{Al}(\text{CoTPhsP})_{\text{ads}}$ (b), and $\text{Mg}_{2.8}\text{Al}(\text{CoTPhsP})_{\text{int}}$ (c).

sion in water). The shoulder around 415 nm is due to the presence of monomeric species isolated in $\text{Mg}_{3.0}\text{Al}(\text{CoTPhsP})_{\text{ads}}$ and $\text{Mg}_{2.8}\text{Al}(\text{CoTPhsP})_{\text{int}}$. Indeed, these species were found in the powder ESR spectra for $\text{Mg}_{3.0}\text{Al}(\text{CoTPhsP})_{\text{ads}}$ and $\text{Mg}_{2.8}\text{Al}(\text{CoTPhsP})_{\text{int}}$ (Figure 8).

The ESR spectrum of CoTPhsP immobilized in the LDHs shows a resonance around 3300 G which is similar to that observed for neat CoTPhsP. As discussed before, this ESR signal is characteristic of the CoTPhsP–O₂ complex. Furthermore, a signal related to the monomeric species was also observed. The ESR spectrum of $\text{Mg}_{2.8}\text{Al}(\text{CoTPhsP})_{\text{int}}$ shows a more resolved signal for this species with $g_{\parallel} = 2.043$ ($A_{\parallel} = 90.5 \times 10^{-4} \text{ cm}^{-1}$) and $g_{\perp} = 2.458$ ($A_{\perp} = 52.6 \times 10^{-4} \text{ cm}^{-1}$), in good agreement with the values found for CoTPhsP monomeric species in DMF/water solution, as reported by de Bolfo et al.^[34] A narrow resonance at $g \approx 2.00$ has also been observed for other cobalt–porphyrins and attributed to a free-radical species^[39] or impurities.^[34,42] Comparing the relative intensities of the monomeric species and CoTPhsP–O₂ complex signals, $\text{Mg}_{2.8}\text{Al}(\text{CoTPhsP})_{\text{int}}$ contains more CoTPhsP molecules in the monomeric form than the corresponding dioxygen complex. In contrast, the latter species is predominant in $\text{Mg}_{3.0}\text{Al}(\text{CoTPhsP})_{\text{ads}}$.

The reactivity of the CoTPhsP complex in solution, intercalated, or adsorbed in the LDH was examined for the decomposition of hydrogen peroxide. Experimental curves of the oxygen released against time are given in Figure 9.

The curve of oxygen evolved obtained at 30 °C and pH = 9.60 (borate-buffered solution) shows a negligible reactivity for $\text{Mg}_{3.0}\text{Al}-\text{CO}_3$ (Figure 9a). The curve for CoTPhsP in homogeneous conditions reveals an oxygen release of 100 μL after 10 min, corresponding to 64% of the H₂O₂ used. Under heterogeneous conditions $\text{Mg}_{2.8}\text{Al}(\text{CoTPhsP})_{\text{int}}$

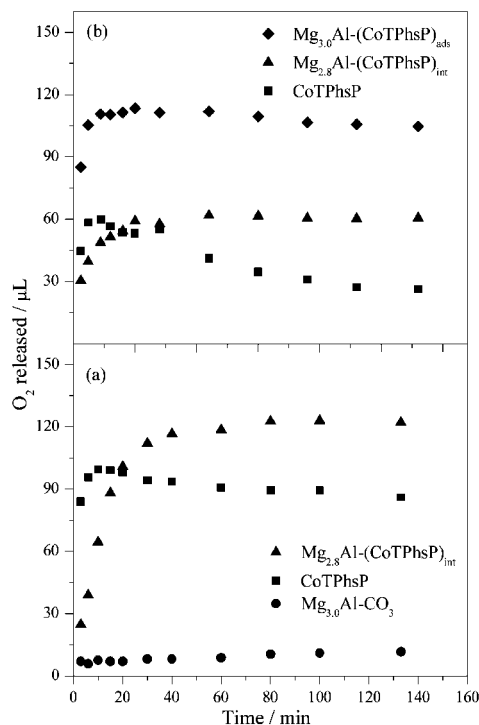


Figure 9. Experimental curves of oxygen released against time for hydrogen peroxide decomposition in the presence of CoTPhsP aqueous solution, $\text{Mg}_{3.0}\text{Al-CO}_3$, $\text{Mg}_{3.0}\text{Al}(\text{CoTPhsP})_{\text{ads}}$, and $\text{Mg}_{2.8}\text{Al}(\text{CoTPhsP})_{\text{int}}$ at 30 °C and pH = 9.60 (a) and 7.80 (b). Other conditions: 13.8 μmol of H_2O_2 and 3.62 μmol of CoTPhsP (a); 14.7 μmol of H_2O_2 and 7.50 μmol of CoTPhsP (b); final volume of 3.00 mL in borate-buffered solution.

was more active, converting 79% (123 μL) of the H_2O_2 . In a second run, we obtained kinetic curves at pH = 7.80 (borate-buffered solution) and 30 °C (Figure 9b). Both CoTPhsP in homogeneous solution and $\text{Mg}_{2.8}\text{Al}(\text{CoTPhsP})_{\text{int}}$ converted about 36% (ca. 60 μL) of the H_2O_2 used. The kinetic curve for $\text{Mg}_{3.0}\text{Al}(\text{CoTPhsP})_{\text{ads}}$ is given in Figure 9b. As can be seen, this sample shows the best activity when compared to CoTPhsP in homogeneous conditions or intercalated into the LDH, converting about 69% (113 μL) of the H_2O_2 .

In both pH = 9.60 and 7.80 buffered solution tests, the H_2O_2 decomposition reaction in the first minutes was faster in the presence of CoTPhsP in homogeneous conditions than $\text{Mg}_{2.8}\text{Al}(\text{CoTPhsP})_{\text{int}}$. After this initial time, the CoTPhsP in solution was deactivated whereas the reaction for intercalated CoTPhsP proceeded. Furthermore, and different from $\text{Mg}_{2.8}\text{Al}(\text{CoTPhsP})_{\text{int}}$ behavior, the H_2O_2 decomposition reaction in the presence of $\text{Mg}_{3.0}\text{Al}(\text{CoTPhsP})_{\text{ads}}$ was faster than the CoTPhsP in solution even during the first few minutes of reaction. Finally, one expects a constant value of the released oxygen content after the maximum conversion, indicating the end of the reaction. However, we noticed a depletion of the oxygen evolved in the reaction with the CoTPhsP in homogeneous conditions.

It is well known that natural porphyrins undergo oxidative degradation by peroxides in the *meso* position.^[43] The second generation of metalloporphyrin catalysts represented by *meso*-substituted porphyrins is considered less lia-

ble to oxidative degradation.^[11] Nevertheless, our results indicate that CoTPhsP may be oxidized during the H_2O_2 decomposition reaction. This finding was corroborated by the UV/Vis spectra obtained from the homogeneous catalyst before and after the reaction. The spectrum (not shown) reveals a lower absorption intensity of the Soret band after the reaction. Another possibility for the oxygen depletion is the formation of an inactive μ -oxo complex (CoTPhsP-O-CoTPhsP) in the course of the H_2O_2 decomposition reaction.^[11] Considering these paths for CoTPhsP deactivation in the presence of H_2O_2 , it is evident that the metalloporphyrin stability is improved when immobilized in the LDHs. In consequence, the CoTPhsP reactivity is further enhanced.

In relation to the different reactivities observed between $\text{Mg}_{2.8}\text{Al}(\text{CoTPhsP})_{\text{int}}$ and $\text{Mg}_{3.0}\text{Al}(\text{CoTPhsP})_{\text{ads}}$, we consider that the CoTPhsP molecules intercalated in the LDH galleries cannot participate in the H_2O_2 decomposition because the intercalation compound is not microporous (N_2 adsorption-desorption isotherm). The active sites should therefore be the CoTPhsP molecules intercalated near the edge sites of the LDH galleries. However, the most important active sites are those located on the external surfaces of the LDH. The CoTPhsP molecules adsorbed on these sites are readily accessible for the H_2O_2 decomposition reaction. We have also observed this enhanced activity for (phthalocyanine)iron(III) tetrasulfonate adsorbed in $\text{Mg}_x\text{Al-CO}_3$ LDHs ($x = 2, 3$, and 4) in the oxidation of catechol.^[44] This feature explains the better reactivity observed for $\text{Mg}_{3.0}\text{Al}(\text{CoTPhsP})_{\text{ads}}$, which contains more available active sites than $\text{Mg}_{2.8}\text{Al}(\text{CoTPhsP})_{\text{int}}$. Moreover, the adsorbed CoTPhsP shows a higher specific surface area (106 m^2g^{-1}) than the intercalated material (34 m^2g^{-1}), which further enhances the reactivity of CoTPhsP in the former.

These findings suggest the use of (tetrasulfonated porphyrin)cobalt immobilized in LDHs as heterogeneous catalysts for the conversion of organic substrates, using H_2O_2 as oxidant. This system is capable of decomposing H_2O_2 (catalase route), but oxidation reactions can be performed by stepwise addition of the oxidant to the system, which minimizes the H_2O_2 decomposition.^[45] Additionally, peroxidation can be predominant or facilitated in the presence of an oxidizable substrate. The porphyrin immobilization in the LDH prevents rapid catalyst deactivation in the presence of the oxidant and provides easy catalyst recovery and re-use.

Conclusions

CoTPhsP has been successfully intercalated and adsorbed in $\text{Mg}_{3.0}\text{Al-CO}_3$ LDH. Infrared spectroscopy indicates that the metalloporphyrin structure is intact after its intercalation and adsorption in the LDHs. The intercalation of CoTPhsP into the LDH changes the crystallinity, thermal stability, and morphology of the resultant materials substantially in relation to the LDH- CO_3 precursor. The surface area and porosity analysis suggest that the material

containing the metalloporphyrin intercalated in LDH has no microporous structure. UV/Vis and electron spin resonance spectroscopy show that the metalloporphyrin immobilized in the LDHs is mainly present in two different forms: the complex formed with molecular oxygen (CoTPhsP-O₂) and the monomeric form (without the dioxygen coordinated).

CoTPhsP is more active and stable in the presence of hydrogen peroxide when the metalloporphyrin is intercalated or adsorbed in the LDHs. The metalloporphyrin adsorbed on the external surfaces of the LDH shows a higher reactivity than the intercalated LDH due to the greater number of active sites available in the former material. Studies involving these materials are underway to test their performance as catalysts for the oxidation of phenols.

Experimental Section

Materials: The reagents Mg(NO₃)₂·6H₂O, Al(NO₃)₃·9H₂O, and Na₂CO₃ were obtained from Aldrich. NaOH was obtained from Merck and 35 % H₂O₂ (w/w) from Peroxidos do Brasil Ltda. (Tetrasulfonated porphyrin)Co^{II} was supplied by Mid Century. All reagents were used as received.

Mg_{3.0}Al-CO₃: The layered precursor containing carbonate ions with an Mg²⁺/Al³⁺ molar ratio of 3 was prepared by co-precipitation of stoichiometric amounts of Mg²⁺ and Al³⁺ in the presence of CO₃²⁻ at pH = 10.0, as described elsewhere.^[30] Chemical analysis confirmed the expected Mg²⁺/Al³⁺ molar ratio of 3.0 and the water content, measured by TGA, of 3.2 H₂O molecules per Al³⁺ cation, which gives the following composition: [Mg_{3.0}Al(OH)_{8.0}](CO₃)_{0.5}·3.2H₂O.

Mg_{2.8}Al(CoTPhsP)_{int}: The intercalation of CoTPhsP into the LDH was conducted as follows: Mg_{3.0}Al-CO₃ (1.0 g, 3.1 mmol) was calcined at 500 °C in air for 4 h; the mixed-metal oxide formed by the thermal decomposition of the LDH was suspended in CoTPhsP solution (130 mL, 4 mmol L⁻¹) using previously decarbonated deionized water, in a Teflon cup. The system was kept in a stainless-steel reactor at 80–85 °C under autogenous pressure for 8 d. The solid was isolated by centrifuging and then washed with decarbonated water until a colorless supernatant was observed. The solid was dried in a desiccator under vacuum with silica gel as drying agent. The following data were found from chemical analysis (C, H, N): C 15.3, H 4.47, N 1.22. Metal analysis indicated Mg²⁺/Al³⁺ and Co²⁺/Al³⁺ molar ratios of 2.80 and 0.09, respectively. The water content measured by TGA was equal to 3.2 H₂O molecules per Al³⁺ cation. The intercalated material contains 231 μmol of CoTPhsP per gram of material.

Mg_{3.0}Al(CoTPhsP)_{ads}: The CoTPhsP was adsorbed on the external surface of Mg_{3.0}Al-CO₃ by suspending it (1.0 g, 3.1 mmol) in CoTPhsP aqueous solution (150 mL, 4 mmol L⁻¹). The suspension was stirred at 80 °C for about 45 h. The sample was washed and dried as described for the intercalated material. Chemical analysis showed that the adsorbed material contains 107 μmol of CoTPhsP per gram of material.

Characterization Techniques: Powder XRD patterns of samples were recorded with a Rigaku diffractometer model Miniflex using Cu-K_α radiation (1.541 Å, 30 kV and 15 mA) and a step of 0.03°.

Specific area data (BET-N₂ method) were determined with a Quantachrome model Quantasorb sorption system after heating

the samples at 200 °C under nitrogen gas flow for 2 h. Porosity analysis was determined from N₂ adsorption-desorption isotherms at liquid nitrogen temperature using a Micromeritics Asap 2010 instrument. Samples were heated at 200 °C under vacuum for 2 h before analysis. Scanning electron micrographs were recorded with an LEO 440i instrument using samples sputter-coated with carbon.

Elemental analysis (C, H, N) was performed with a Perkin–Elmer model 2400 analyzer. Magnesium, aluminum and cobalt contents in the LDH samples were determined with a Spectro Analytical Instruments ICP emission spectrometer. Thermogravimetric analysis (TGA) was carried out with a Shimadzu TGA-50 instrument under synthetic air (flow rate = 50 mL min⁻¹) at a heating rate of 10 °C min⁻¹ up to 900 °C.

FT-IR spectra of samples in KBr matrix were recorded with a MIDAC model PRS-INT series 192 spectrometer or a Perkin–Elmer model 1750 spectrometer, in the range 4000–400 cm⁻¹. UV/Vis spectra were recorded with a Shimadzu model UV-2401PC spectrophotometer. For spectral acquisition of CoTPhsP solutions at high concentration (> 0.1 mmol L⁻¹), an aliquot of the solution (5 μL) was placed between two 1.25-mm-thick quartz rectangular windows (45 × 12.5 mm) and firmly fastened together in a holder for cells with detachable windows. Solid samples were dispersed in deionized water or water/DMF mixtures and the spectra recorded with the same spectrophotometer equipped with an integration sphere. ESR experiments were conducted with a Bruker ER 200D-SRC instrument, operating at X-band (ca. 9.5 GHz), and using DPPH (*α,α*-diphenyl-β-picrylhydrazyl) for calibration. Instrumental standard conditions for the measurements were: frequency = 9.48 GHz, microwave power = 20 mW, modulation frequency = 100 kHz, modulation amplitude = 15 G, at liquid nitrogen temperature (77 K).

Reactivity Tests with Hydrogen Peroxide: The reactivity and stability of the CoTPhsP in homogeneous conditions and immobilized in the LDHs towards hydrogen peroxide decomposition were evaluated by monitoring the released molecular dioxygen with a Warburg apparatus from B. Brown, model V-85, at a constant temperature (30 °C). The experiments were carried out at two different pHs in borate-buffered solutions (12.5 mmol L⁻¹). In the first run at pH = 9.60, CoTPhsP (0.30 mL of a 12.5 mmol L⁻¹ solution), Mg₃Al-CO₃ (8.1 mg), and Mg_{2.8}Al(CoTPhsP)_{int} (16.9 mg) were added to hydrogen peroxide (2.70 mL of a 5.12 mmol L⁻¹ solution). In the second run at pH = 7.80, CoTPhsP (0.30 mL of a 25.0 mmol L⁻¹ solution), Mg_{2.8}Al(CoTPhsP)_{int} (34.7 mg) or Mg_{3.0}Al(CoTPhsP)_{ads} (70.3 mg) were added to hydrogen peroxide (2.70 mL of a 5.44 mmol L⁻¹ solution). Borate-buffered solution was used to complete the volume to 3.00 mL under the heterogeneous conditions. Each experiment was conducted in duplicate and the amounts of CoTPhsP were the same for both homogeneous and heterogeneous conditions. In order to certify that leaching of CoTPhsP was not taking place under the heterogeneous conditions, at the end of the tests, samples were taken and filtered through 0.22 μm disposable filters (Millipore). UV/Vis spectra of the filtered solutions were registered to check for the presence of free CoTPhsP, which was negative for all runs.

Acknowledgments

The authors are grateful to FAPESP and CNPq (Brazilian agencies) for financial support and fellowships. We also thank Dr. Antonio Carlos V. Coelho (EP-USP) for measuring the N₂ adsorption-desorption isotherms.

- [1] G. Alberti, U. Costantino, in *Solid State Supramolecular Chemistry: Two- and Three-Dimensional Inorganic Networks* (Eds.: G. Alberti, T. Bein), Pergamon, New York, **1996**, vol. 7, p. 1.
- [2] J.-H. Choy, *J. Phys. Chem. Solids* **2004**, *65*, 373–383.
- [3] F. Trifirò, A. Vaccari, in *Solid State Supramolecular Chemistry: Two- and Three-Dimensional Inorganic Networks* (Eds.: G. Alberti, T. Bein), Pergamon, New York, **1996**, vol. 7, p. 251.
- [4] P. S. Braterman, Z. P. Xu, F. Yarberry, in *Handbook of Layered Materials* (Eds.: S. M. Auerback, K. A. Carrado, P. K. Dutta), Marcel Dekker, New York, **2004**, p. 373.
- [5] A. de Roy, C. Forano, K. El Malki, J. P. Besse, in *Expanded Clays and Other Microporous Solids* (Eds.: M. L. Occelli, H. E. Robson), Van Nostrand Reinhold, New York, **1992**, vol. 2, p. 108.
- [6] B. F. Sels, D. E. de Vos, P. A. Jacobs, *Catal. Rev.* **2001**, *43*, 443–488.
- [7] F. Leroux, J. P. Besse, *Chem. Mater.* **2001**, *13*, 3507–3515.
- [8] N. K. Lazaridis, A. Hourzemanoglou, K. A. Matis, *Chemosphere* **2002**, *47*, 319–324.
- [9] A. I. Khan, D. O'Hare, *J. Mater. Chem.* **2002**, *12*, 3191–3198.
- [10] J.-H. Choy, S.-Y. Kwak, J.-S. Park, Y.-J. Jeong, J. Portier, *J. Am. Chem. Soc.* **1999**, *121*, 1399–1400.
- [11] B. Meunier, *Chem. Rev.* **1992**, *92*, 1411–1456.
- [12] C. Walling, *Acc. Chem. Res.* **1975**, *8*, 125–131.
- [13] D. E. de Vos, B. F. Sels, P. A. Jacobs, in *Advances in Catalysis* (Eds.: B. C. Gates, H. Knözinger), Academic Press, New York, **2001**, vol. 46, p. 1.
- [14] R. A. Sheldon, I. W. C. E. Arends, H. E. B. Lemmers, *Catal. Today* **1998**, *41*, 387–407.
- [15] L. Barloy, J. P. Lallier, P. Battioni, D. Mansuy, Y. Piffard, M. Tournoux, J. B. Valim, W. Jones, *New J. Chem.* **1992**, *16*, 71–80.
- [16] D. S. Robins, P. K. Dutta, *Langmuir* **1996**, *12*, 402–408.
- [17] T. Shichi, Z. Tong, S. Hirai, K. Takagi, *Chem. Lett.* **2002**, *31*, 834–835.
- [18] M. Halma, F. Wypych, S. M. Drechsel, S. Nakagaki, *J. Porphyrins Phthalocyanines* **2002**, *6*, 502–513.
- [19] Z. Tong, T. Shichi, K. Takagi, *Mater. Lett.* **2003**, *57*, 2258–2261.
- [20] S. Y. Ryu, M. Yoon, J.-H. Choy, S. H. Hwang, A. Frube, T. Asahi, H. Masuhara, *Bull. Korean Chem. Soc.* **2003**, *24*, 446–452.
- [21] Z. Tong, T. Shichi, G. Z. Zhang, K. Takagi, *Res. Chem. Intermed.* **2003**, *29*, 335–341.
- [22] F. Wypych, G. A. Bubniak, M. Halma, S. Nakagaki, *J. Colloid Interface Sci.* **2003**, *264*, 203–207.
- [23] I. Y. Park, K. Kuroda, C. Kato, *Chem. Lett.* **1989**, *11*, 2057–2058.
- [24] S. Bonnet, F. A. de Roy, J. P. Besse, P. Maillard, M. Momen-teau, *Chem. Mater.* **1996**, *8*, 1962–1968.
- [25] H. Tagaya, A. Ogata, T. Kuwahara, S. Ogata, M. Karasu, J. Kadokawa, K. Chiba, *Microporous Mater.* **1996**, *7*, 151–158.
- [26] S. Miyata, *Clays Clay Miner.* **1975**, *23*, 369–375.
- [27] T. S. Srivastava, M. Tsutsui, *J. Org. Chem.* **1973**, *38*, 2103–2103.
- [28] F. Cavani, F. Trifirò, A. Vaccari, *Catal. Today* **1991**, *11*, 173–301.
- [29] S. K. Yun, V. R. L. Constantino, T. J. Pinnavaia, *Microporous Mater.* **1995**, *4*, 21–29.
- [30] C. A. S. Barbosa, A. M. D. C. Ferreira, V. R. L. Constantino, A. C. V. Coelho, *J. Incl. Phenom. Macrocycl. Chem.* **2002**, *42*, 15–23.
- [31] V. R. L. Constantino, T. J. Pinnavaia, *Inorg. Chem.* **1995**, *34*, 883–892.
- [32] K. S. W. Sing, D. H. Everett, R. A. W. Haul, L. Moscou, R. A. Pierotti, J. Rouquerol, T. Siemieniowska, *Pure Appl. Chem.* **1985**, *57*, 603–619.
- [33] M. Gouterman, in *The Porphyrins* (Ed.: D. Dolphin), Academic Press, New York, **1979**, vol. 3, p. 1.
- [34] J. A. de Bolfo, T. D. Smith, J. F. Boas, J. R. Pilbrow, *J. Chem. Soc., Dalton Trans.* **1976**, 1495–1500.
- [35] F. A. Walker, *J. Magn. Reson.* **1974**, *15*, 201–218.
- [36] F. A. Walker, *J. Am. Chem. Soc.* **1970**, *92*, 4235–4244.
- [37] J. Subramanian, in *Porphyrins and Metalloporphyrins* (Ed.: K. M. Smith), Elsevier Scientific, Amsterdam, **1975**, p. 555.
- [38] I. V. Ruzic, T. D. Smith, J. R. Pilbrow, *J. Chem. Soc., Dalton Trans.* **1981**, 2365–2369.
- [39] D. F. Evans, D. Wood, *J. Chem. Soc., Dalton Trans.* **1987**, 3099–3101.
- [40] J. A. Shelnutt, M. M. Dobry, J. D. Datterlee, *J. Phys. Chem.* **1984**, *88*, 4980–4987.
- [41] W. Xu, H. Guo, D. L. Akins, *J. Phys. Chem. B* **2001**, *105*, 1543–1546.
- [42] J. A. Assour, W. K. Kahn, *J. Am. Chem. Soc.* **1965**, *87*, 207–212.
- [43] S. B. Brown, H. Hatzikonstantinou, D. G. Herries, *Biochem. J.* **1978**, *174*, 901–907.
- [44] C. A. S. Barbosa, P. M. Dias, A. M. D. C. Ferreira, V. R. L. Constantino, *Appl. Clay Sci.* **2005**, *28*, 147–158.
- [45] A. Hadasch, A. Sorokin, A. Robion, B. Meunier, *New J. Chem.* **1998**, *22*, 45–51.

Received: October 15, 2004